

# RSC Advances



This is an *Accepted Manuscript*, which has been through the Royal Society of Chemistry peer review process and has been accepted for publication.

*Accepted Manuscripts* are published online shortly after acceptance, before technical editing, formatting and proof reading. Using this free service, authors can make their results available to the community, in citable form, before we publish the edited article. This *Accepted Manuscript* will be replaced by the edited, formatted and paginated article as soon as this is available.

You can find more information about *Accepted Manuscripts* in the [Information for Authors](#).

Please note that technical editing may introduce minor changes to the text and/or graphics, which may alter content. The journal's standard [Terms & Conditions](#) and the [Ethical guidelines](#) still apply. In no event shall the Royal Society of Chemistry be held responsible for any errors or omissions in this *Accepted Manuscript* or any consequences arising from the use of any information it contains.

**Layer-by-Layer self-assembled thin films by chitin fiber and heparin with anti-thrombus characteristics**

*Taihei Taniguchi, Kyu-Hong Kyung, Seimei Shiratori\**

<sup>1</sup>Grad. Sch. Sci. Tech., Keio Univ., 3-14-1 Hiyoshi, Kohoku-ku, Yokohama, JAPAN.

*\*shiratori@appi.keio.ac.jp*

**Tel: +81-45-566-1602**

**Fax: +81-45-566-1602**

**Abstract**

Anti-thrombus coatings using natural polymers with high biocompatibility were successfully fabricated by a Layer-by-Layer (LbL) method. The cationic and anionic components were chitin nanofibers and heparin, respectively. LbL multilayers were successfully fabricated by depositing different numbers of bilayers. Analyzing the damping waves of Quartz Crystal Microbalance (QCM) measurements showed that the film hardened as the number of bilayers deposited increased. Mass change measurements via QCM, scanning electron microscopy, atomic force microscopy, ellipsometry, and X-ray photoelectron spectroscopy were also carried out. The density of the chitin nanofiber layers increased as the number of bilayers increased. Simultaneously, the film stability in solution improved. The fabricated 30-bilayer film showed a fibrous structure on its surface and no structural disorder, even after 48 hours immersion in phosphate buffered saline (PBS), so high stability in PBS was demonstrated. The anti-thrombus properties of the film were also investigated by measuring the amount of fibrinogen adsorbed using QCM. This film not only inhibits fibrinogen adsorption, but those fibrinogen which do adsorb detach relatively easily (compared with fibrinogen adsorbed onto an uncoated QCM substrate). Furthermore, while the uncoated glass substrate adsorbed a large quantity of blood on its surface, the 30-bilayer coated glass substrate successfully inhibited blood adsorption and blood solidification.

## Introduction

Recently, coatings which prevent thrombus formation are attractive for developing medical equipment, such as stents and artificial blood vessels. Thrombus formation, which causes secondary disease, often occurs on artificial materials in the human body. [1] Thrombus formation begins with attachment of platelets, followed by adhesion of fibrinogens (which are proteins), and formation of a fibrinogen network which aggregates the platelets. Therefore, adsorption of fibrinogens on surfaces causes thrombus formation, and sometimes reduces the sensitivity and/or efficacy of devices inside our body. [2-4]

Previous studies show that some materials, such as poly ethylene glycol (PEG) and poly acrylic acid, can be used to make coatings which suppress thrombus formation. PEG, a hydrophilic macromolecule with a long polymer chain, is effective at preventing fibrinogen adhesion because of the entropic and steric repulsive forces arising when the polymer molecules are compressed by protein molecules approaching the surface. [5-9]

Layer-by-Layer (LbL) assembly was first developed by Decher and coworkers in the early 1990s. [10-13] The LbL assembly method has attracted much attention because of its versatility and convenience. [13, 14] LbL assembly can be achieved by the alternate immersion of certain materials into solutions of oppositely charged, water-soluble polymers; [15-18] this alternately forms polyion complexes on the substrate surface to create ultrathin polymeric films. Moreover, LbL assembly allows the surface structure and thickness of a film to be controlled on micro- and nanoscales. There have been various applications of LbL assembly, including for antireflective and superhydrophobic coatings, dye release and drug delivery systems.[19-25] We also reported that antithrombogenicity was achieved with polyelectrolyte multilayer thin film prepared from poly(vinyl alcohol)-poly(acrylic acid) (PVA-PAA) blends, deposited in alternate layers with poly(allylamine hydrochloride) (PAH).[26]

For medical applications, such as stents and artificial blood vessels, it is critical that the coating not only inhibit thrombus formation, but also be highly biocompatible and mechanically durable. Sheng Meng and coworkers developed chitosan-heparin LbL coatings which promoted endothelialization, and showed high biocompatibility and anticoagulation characteristics. [27] Yao Shu and coworkers deposited LbL multilayers of chitosan and heparin on titanium substrates. The multilayers are beneficial to cytobiocompatibility. [28] Also, Maria Bulwan and coworkers developed one-component chitosan-based ultrathin films fabricated using LbL technique, which may be potentially

useful for many biomedical and environmental protection applications. [29] Chitosan and heparin (HEP) is both biopolymers. Chitosan is a natural cationic polysaccharide, widely studied and used as a matrix for tissue engineering and drug release because of its good biocompatibility and biodegradability. Crab shells show high tensile strength and bendability [30,31], and thus chitin nanofibers (CHNFs) purified from crab shells and partially transformed from chitin to chitosan by deacetylation have also attracted much attention because of their high potential to show mechanical strength in addition to the advantageous characteristics of chitosan. HEP is biocompatible and widely used in medical applications, where it shows strong anti-thrombus characteristics. For example, it strongly inhibits sub-acute in-stent thrombus formation. [32-34] There are many reports of anti-thrombus coatings using HEP prepared by LbL-assembly methods. [35, 28] However, these studies did not evaluate the film stability.

In the present research, to take advantage of the biocompatibility of the two polysaccharides, and combine the mechanical stability of CHNFs and anti-thrombus characteristics of HEP, new CHNFs/HEP LbL-assembly multilayers were deposited on glass substrates. Each polymer deposition step was evaluated by a Quartz Crystal Microbalance (QCM); the QCM was also used to determine fibrinogen adsorption and detachment abilities. QCM is often used to investigate protein adsorption, lipids and membranes, cells, DNA, and carbohydrates, and in applications within polymer physics. [36, 37] Furthermore, from differences in the rate of decay of the oscillation wave after turning off the voltage of the QCM, we evaluated the relative harnesses of the films. The films were also characterized by X-ray photoelectron spectroscopy (XPS), scanning electron microscopy (SEM), and atomic force microscopy (AFM). The anti-thrombus performance was evaluated indirectly measuring fibrinogen adsorption and detachment in PBS solution, and directly from the mass of blood that adhered to the coated and uncoated surfaces.

## Materials and Methods

### Material

CHNFs were purified from crab shell. Heparin sodium (from porcine intestinal mucosa, 14.4 kDa, 12.5 % sulfone) and fibrinogen were purchased from Wako Pure Chemical (Osaka, Japan). Poly (diallyl dimethyl ammonium chloride) (PDDA,  $M_w$  200,000-350,000 10 mM aqueous solution) Poly (4-styrenesulfonic acid sodium salt) (PSS,  $M_w$  70,000 10 mM aqueous solution) and phosphate buffered saline (PBS) were from Sigma-Aldrich Japan(Tokyo, Japan). Pig blood was purchased from Shibaura Zoki industry (Tokyo, Japan).

All experiments were conducted in air at ambient temperature and used ultra-pure water (Aquarius GS-500.CPW, Advantec, Tokyo, Japan, 18.2 MΩ); the pH values of the dipping solutions for the LbL method were adjusted using sodium hydroxide and acetic acid.

### **Refinement of CHNFs**

The CHNFs were fabricated from dried crab shell powder according to methods described in the literature. [31, 38] Firstly, the crab shell powder was treated using 2 M HCl solution for 2 days at room temperature to remove mineral salts. After rinsing with an abundance of ultra-pure water, the treated chitin powder was refluxed in 2 M NaOH solution for two days to remove fibrinogens. Next, the pigments in the sample were removed using 1.7 wt. % NaClO<sub>2</sub> in buffer solution; this treatment was applied for 6 h at 80 °C. The sample was rinsed thoroughly with distilled water, then suspended in 33 wt.% NaOH containing 0.03 g NaBH<sub>4</sub>, as described in a previous study. [39] The CHNF solution was diluted to a concentration of 0.025 wt.%.

### **Preparation of Layer-by-Layer multilayers**

CHNFs and HEP solutions were prepared by direct dissolution in ultra-pure water to a final concentration of 0.25 and 2 mg/mL, respectively. Since heparin has higher anti-thrombus ability, we adjusted the higher concentration value for heparin. The pH values of the cationic and anionic solutions were 4.0 in all experiments (Supporting information 1). Glass substrates were cleaned by ultrasonication for 5 min in ultra-pure water followed by ultrasonication for 2 min in potassium hydroxide solution (1:120:60 wt. % KOH/H<sub>2</sub>O/IPA), and rinsed twice by ultrasonication in water as above. The sequence for multilayer construction was as follows: the hydroxylated glass substrate was immersed in CHNFs solution for 15 min, which changes the surface charge to positive, and then rinsed three times in ultra-pure water for 1 min. Then the sample was exposed to negatively-charged HEP solution for 15 min, which changes the surface charge to negative again, followed by the same rinsing procedure and dried at natural condition. The cycle of immersing the substrate into CHNFs and HEP solutions alternately was repeated n times to obtain the desired film. To increase the anti-thrombus ability, we use heparin to the outermost layer, because heparin is the key material for the film to show anti-thrombus ability. The ultrathin films containing n alternating layers of CHNFs and HEP were defined as (CHNFs/HEP) n.

### **Film characterization using QCM**

QCM measurements were used to measure the mass of each polyelectrolyte adsorption in polymer solution and fibrinogen adsorption in PBS solution. The QCM used in our study is AT-cut quartz with gold electrode. In this study, the oscillation circuit was fabricated by ourselves. The oscillation circuit is Hartley type because this type is very stable to measure the film and protein adsorption in liquid. Then we convert the frequency shift to the adsorption mass by Sauerbrey formula and Gordon-Kanazawa formula. [40, 41] Moreover, we analyzed the damping waves of the QCM at the time turning off the circuit using an oscilloscope (GDS-1152A-U Instek, Kanagawa, Japan), and evaluated the relative hardness of each film with different number of bilayers. In this paper, we called the film with low viscoelasticity as “hard film” and the film with high viscoelasticity as “soft film” The fundamental resonant frequency of the crystal was 10 MHz and a gold electrode was used. The crystal was mounted with one side exposed to the solution. Before LbL assembly, a buffer layer consisting of (PDDA/PSS)<sub>5</sub> bilayers was first deposited onto each QCM substrate. Each QCM surface structure shows individual difference, so in order to arrange surface structure; PDDA/PSS were fabricated as the buffer layer. Since PDDA and PSS are both strong electrolytes, PDDA/PSS LbL film are known to become very thin film. Therefore, PDDA/PSS LbL film was found to be suitable for buffer layer.

#### **Microscopic Analysis and Film characterization**

The structure and morphology of the multilayer films were observed by SEM (STS, Philips XL-30 SEM, MA, North Billerica, USA) and AFM (Bruker AXS, Kanagawa, Japan). The film thicknesses were evaluated by ellipsometry measurements using Mary-103(Five lab, Kawaguchi Japan). LbL thickness measurements were carried out in air at ambient temperature. The elements within the polyelectrolyte multilayers formed on glass were analyzed using XPS (JEOL, JPS-9010, Tokyo, Japan).

#### **Investigation of multilayer stability**

The CHNFs/HEP multilayers are being developed for in vivo use. The static stability of CHNFs/HEP multilayers on 1 square centimeter was studied by immersing the films into 100ml PBS for up to 48 h, and observing any changes in the films after this time.

#### **Fibrinogen adhesion testing**

Fibrinogen is thought to be the first factor protein in blood coagulation; it forms a net of fibrous matter called fibrin in the final stage of the mechanism of blood coagulation. Thus, QCM measurements of fibrinogen adsorption were used to quantify the anti-thrombus performance of the films. Fibrinogen was dissolved into PBS to a final

concentration of 2 mg/mL. A quartz substrate, coated with a multilayer film, was dipped into PBS for 10 min to stabilize the frequency of the quartz, followed by dipping into fibrinogen solution for 1 h to measure the mass of fibrinogen adsorbed to the quartz. After 1 h, the quartz on which fibrinogen had adsorbed was dipped into PBS for 10 min and the mass of the previously adsorbed fibrinogen that desorbed was measured – this mass change can be used as an index of the strength of the adsorptive interaction between the fibrinogen and the film.

### **Blood Anticoagulation testing**

Pig blood was prepared for the anticoagulation test. 80  $\mu$ l of blood were cast onto non-coated and film-coated glass (1 $\times$ 1 cm) substrates; the substrates were then incubated in air at 37  $^{\circ}$ C for 15 min. After 15 min, the each substrate was rinsed vigorously with ultra-pure water.

### **Results and Discussion**

#### **Layer-by-Layer Assembly of CHNFs and HEP.**

The CHNF solution was diluted to a concentration of 0.025 wt. %. Figure 1 shows the AFM image of the surface structure of the film fabricated by casting method using 0.025 wt. % CHNFs water solution on a glass substrate. We call “cast film of CHNF” hereafter. Very fine CHNFs (~39 nm in diameter) were observed. These fine CHNFs were used as the cationic material in this study.

LbL assembly by alternating electrostatic adsorption of CHNFs and HEP occurs as illustrated schematically in Figure 2. Figure 3 shows the adsorbed mass of fibrinogen to the QCM, which was calculated by the frequency shift decreased with increasing amount of polymer adsorbed on the surface of QCM substrate, plotted against the steps of the CHNFs/HEP LbL assembly. The stepwise polymer depositions are shown from the decrease in frequencies of QCM as assembly proceeds. The total thicknesses of the prepared CHNFs/HEP films were 73.7 nm for 10 bilayers and 350.2 nm for 30 bilayers.

When the deposition time was 3 minutes for each layer, a homogeneous LbL film was not formed. We consider that such a short adsorption time resulted in unstable and slow adsorption during the deposition (Supporting information 2). Sufficient adsorption time (such as 15 minutes) is required for stable deposition.

AFM images of the surface structures of (CHNFs/HEP)<sub>n</sub> films with n=10, 20, 30 and 50 are shown in Figure 4. Though the top views of 10-bilayer and 20-bilayer films have less fibrous structure, the 30-bilayer film showed a complex, intertwined, fibrous structure, derived from CHNFs. Also about 50 bilayer, the groups of the fiber structure can also be confirmed extensively, which is also indicated by the RMS values. Our

suggested reasons for this fibrous structure appearing on the top of the films containing more bilayers are as follows: in the early stages of LbL adsorption, the surface of the film has a nearly flat structure (because there has been less adsorption); this means that it also has a relatively small specific surface area, and a low amount of electrostatic charge. However, as the number of bilayers increases, the increasing mass of material adsorbed makes the surface rougher, increasing the specific surface area and meaning that there is more charge on this surface than on the earlier-stage surface. This observation is consistent with the RMS values measured by AFM (10 bilayer: 7.53 nm, 20 bilayer: 10.4 nm, 30 bilayer: 12.4 nm, 50 bilayer: 39.9 nm). This larger quantity of electrostatic charge causes numerous CHNFs to adsorb onto the film. Unless otherwise noted, all subsequent experiments used 30-bilayer films.

The XPS spectra of (CHNFs/HEP)<sub>30</sub> LbL films are shown in Figure 5. Sulfone group peaks are observed, confirming that HEP exists on the top of the film. The two peaks are derived from the S2s and S2p orbitals of the sulfone. It is important that the sulfone groups of HEP are located on the surface of the films, because they are expected to play an important role in the antithrombogenic activity of the multilayer films. QCM results that are related to the film density and hardness are shown in Figure 6. These damping waves are for non-coated, buffer only coated, the 30-bilayer coated, the 50-bilayer coated, cast film of CHNFs, respectively. The damping time for each QCM wave becomes shorter for the high viscoelasticity films, because higher viscoelasticity films absorb more vibration than lower films. [42, 43, 44] For this measurement, we evaluated the films by the simple QCM-D system used a digital storage oscilloscope and UNIX programs for analyzing the  $2 \times 10^6$  (2M) plots stored in the oscilloscope. We used Cygwin UNIX for Windows for large-data-set analysis techniques to obtain QCM-D frequency information and for the determination of viscoelasticities of stacked film made of soft materials [44].

Therefore, observing the damping behavior of the vibration of the quartz which coated the film, relative viscosity of the film, which lead to the hardness, is easily found. The results are shown in Figure 6. Non-coated QCM, which is metal surface, is the hardest, therefore its damping time is the longest. As shown in the figure, as the number of bilayers increased, the damping time of the QCM wave became longer. The values of the dissipation of buffer only coated, 30 bilayer coated and 50 bilayer coated ( $D \times 10^6$  where  $D = \frac{1}{\pi f \tau}$  is dissipation factor of the films;  $f$  is characteristic frequency of the quartz (10MHz) and  $\tau$  is the relaxation time of the decaying amplitude) was  $6.38 \times 10^{-4}$ ,  $6.47 \times 10^{-4}$  and  $5.99 \times 10^{-4}$ , respectively. This means that the LbL films in our study became lower viscoelasticity as the number of bilayers increased. We consider that this phenomenon was caused by accretion of high mechanical strength CHNFs into the film as the number of bilayers increased and imply that the

films with more bilayers should have higher stability due to the high mechanical strength of CHNFs. By CHNFs first adsorbing onto the PDDA/PSS buffer layer, the film became hard, so the uncoated (buffer coated) film is relatively high viscoelastic and reveals lowest oscillation time. The AFM images in Figure 4 also show a more extensive nanofiber structure as the number of bilayers increases – this would result in increased film strength. Hardness of CHNFs was demonstrated by the damping wave of the cast film of CHNFs. The damping time of the cast film of CHNFs is longer than that of PDDA/PSS polymer coating and the 30 bilayers LbL coating. However, compared with 50 bilayers coatings, the cast film of CHNFs was found to be soft because of the short damping times. One reason of this is the mass difference of adsorbed polymer. The weight of 50 bilayer (CHNFs/HEP) LbL coating was 4860 ng, which was estimated from QCM data of Figure 3, while that of the cast film of CHNFs was 7365 ng. Therefore, the cast film of CHNFs, which is larger amount of adsorbed mass, became softer than 50 bilayer LbL coating. Moreover, which is more important, the other reason is the adsorbing force between the layer materials. The cast film of CHNFs was adsorbed onto the QCM surface by van der Waals force, on the other hand, the 50 bilayer LbL coating was formed by the electrostatic force between CHNFs and HEP. In other words, it may suggest that electrostatic interaction between CHNFs and HEP is the main difference that improves coating “hardness” as opposed to CHNFs as a cast film. For this point of view, we tried to fabricate the cast film by CHNFs and HEP mixed solution, however, the polyion complex formed precipitation on substrate and the numerous aggregated complex particles did not form uniform film. We consider that LbL method is very effective to form uniform film by CHNFs and HEP and the formed (CHNFs/HEP) LbL coating was harder than that of the cast film of CHNFs because the electrostatic force is stronger than the van der Waals force.

From these experimental results and considerations, we concluded that the stability of (CHNFs/HEP) LbL film are caused by the usage of CHNFs and LbL fabrication method based on electrostatic force.

SEM images after immersion of the (CHNFs/HEP)<sub>30</sub> in PBS are shown in Figure 7. As shown in the figure, fibrous structures derived from CHNFs are not degraded by immersion in PBS. This indicates that the films are durable enough to be potentially useful *in vivo*. Even after immersion for 48 h, there is no damage to the CHNFs, although the fibrous structure swelled a little with the diameter of CHNFs increasing from ~48 nm before immersion to ~69 nm after 48 h immersion, which was measured from SEM image and by using image-J software. This stability probably results from both the strength of the original CHNFs (purified from hard crab shell) and the complicated entanglement of the fibers.

The masses of fibrinogen adsorbed onto different surfaces are shown in Figure 8. The amount of fibrinogen adsorbed on the LbL film was less than half that adsorbed on a non-coated QCM substrate. Also, while it took 2 min 30 s for the non-coated QCM substrate to acquire 80% of its final mass of adsorbed fibrinogen, it took 32 min for the (CHNFs/HEP)<sub>30</sub> film-coated QCM substrate. This fibrinogen-resistance property is thought to be caused by the negatively charged sulfone groups of HEP, which show anticoagulation ability. The sulfate group of heparin is highly negatively charged, and we consider that fibrinogen which mainly has negative charge likely to repel by the negative charge of heparin by electrostatic interaction, and thus result in the lower adsorption of fibrinogen on to the QCM electrode which were covered by (CHNFs/HEP)<sub>30</sub> film.

Moreover, Figure 9 shows the fibrinogen detachment from the LbL films when they are rinsed (after being dipped for 10 min in fibrinogen solution). The fibrinogens adsorbed onto the LbL film are detached more easily than those adsorbed onto the non-coated QCM substrate; this implies that the CHNFs/HEP LbL films can not only reduce fibrinogen adsorption but also weaken the interaction between the fibrinogen and the surface.

Finally the anti-thrombus property of the multilayer film was examined. The results are shown in Figure 9. As described in the section of “Blood Anticoagulation testing”, pig blood was prepared for the anticoagulation test. 80  $\mu$ l of blood were cast both onto non-coated glass and film-coated glass (1 $\times$ 1 cm) substrates simultaneously; the substrates were then incubated in air at 37  $^{\circ}$ C for 15 min. After 15 min, the each substrate was rinsed vigorously using a plastic syringe with 10ml of ultra-pure water. The results are shown in Figure 10, while much blood adhered to the non-coated substrate, on the other hand, only a small amount of blood (less than 0.5  $\mu$ l) adhered to the LbL-coated substrate. From these results, we can confirm that the CHNFs/ HEP LbL multilayers have anti-thrombus properties.

## Conclusion

We demonstrated a method for fabricating anti-thrombus films via LbL self-assembly of CHNFs and HEP polyelectrolyte multilayers. Fibrous structure of CHNFs emerged on the surface of the films as the number of bilayers increased. The films inhibit fibrinogen adsorption, and any adsorbed fibrinogen is easily detached; this prevents blood from coagulating on glass substrates coated with the films. Furthermore, the films with more bilayers should have higher stability due to the high mechanical strength of CHNFs and also its strength arise from electrostatic force of LbL method, which can be concluded from damping waves of oscillating circuit for QCM

substrates, and have high stability in PBS, which indicates that they might also be stable in the body. We considered that the combination of the hardness CHNFs purified from crab shells and LbL method are very important factors for the stability of thin films. The multilayers fabricated in this study have potential to be used in medical applications such as stents and artificial blood vessels.

## Reference

1. Ratner BD. *Biomaterials Science. An Introduction to Materials in Medicine*, 2nd ed.; Elsevier Academic Press: Boston, 2004.
2. Donlan RM. Biofilm Formation: A Clinically Relevant Microbiological Process. *Clin. Infect. Dis.* 2001;33:1387-1392.
3. Peng Wu, David W. Drug/device combinations for local drug therapies and infection prophylaxis. *Biomaterials* 2006;27:2450-2467.
4. Pavithra D, Doble M. Biofilm formation, bacterial adhesion and host response on polymeric implants—issues and prevention. *Biomed. Mater.* 2008;3:034003-034015.
5. Prime KL, Whitesides GM. Self-Assembled Organic Monolayers: Model Systems for Studying Adsorption of Proteins at Surfaces. *Science* 1991;252:1164-1167.
6. Prime KL, Whitesides GM, Adsorption of Proteins Oligo(ethylene oxide): A Model System Using Self-Assembled. *J. Am. Chem. Soc.* 1993;115:10714-10721.
7. Jeon SI, Lee JH, Andrade JD, Degennes PG. Protein—surface interactions in the presence of polyethylene oxide: I. Simplified theory. *J. Colloid Interface Sci.* 1991;142:149-158.
8. McPherson T, Kidane A, Szleifer I, Park K. Prevention of protein adsorption by tethered poly(ethylene oxide) layers: Experiments and single-chain mean-field analysis. *Langmuir* 1998;14:176-186
9. Fang F, Satulovsky J, Szleifer I. Kinetics of Protein Adsorption and Desorption on Surfaces with Grafted Polymers. *Biophys. J.* 2005;89:1516-1533.
10. Decher G, Hong J. BUILDUP OF ULTRATHIN MULTILAYER FILMS BY A SELF-ASSEMBLY PROCESS, 1 CONSECUTIVE ADSORPTION OF ANIONIC AND CATIONIC BIPOLAR AMPHIPHILES ON CHARGED SURFACES. *Chem., Macromol. Symp.* 1991;46:321-327.

11. Decher G, Hong JD, Schmit J. Buildup of ultrathin multilayer films by a self-assembly process III. Consecutively alternating adsorption of anionic and cationic polyelectrolytes on charged surfaces. *Thin Solid Film* 1992;210-211:831-835.
12. Lvov Y, Decher G, Möhwald H. Assembly, Structural Characterization, and Thermal Behavior of Layer-by-Layer Deposited Ultrathin Films of Poly(vinyl sulfate) and Poly(allylamine). *Langmuir* 1993;9:481-486
13. Decher G. Fuzzy Nanoassemblies Toward Layered Polymeric Multicomposites. *Science* 1997;277:1232-1237.
14. Zhang X, Shen JC. Self-Assembled Ultrathin Films From Layered Nanoarchitectures to Functional Assemblies. *Adv. Mater.* 1999;11:1139-1309.
15. Decher G. Compr. Layered nanoarchitectures via directed assembly of anionic and cationic molecules. *Supramol. Chem.* 1996;9:507-528.
16. Knoll W. Self-assembled microstructures at interfaces. *Curr. Opin. Colloid Interface Sci.* 1996;1:137-143.
17. Hammond PT. Recent explorations in electrostatic multilayer thin film assembly. *Curr. Opin. Colloid Interface Sci.* 1999;4:430-442.
18. Bertrand P, Jonas A, Laschewsky A, Legras RM. Ultrathin polymer coatings by complexation of polyelectrolytes at interfaces suitable materials, structure and properties. *Rapid Commun.* 2000;21:319-348.
19. Lu Y, Choi YJ, Lim SH, Kwak D, Shim C, Lee SG, Cho K. pH-Induced Antireflection Coatings Derived From Hydrogen-Bonding-Directed Multilayer Films. *Langmuir* 2010;26:17749- 17755.
20. Zhang L, Sun J. Layer-by-Layer Codeposition of Polyelectrolyte Complexes and Free Polyelectrolytes for the Fabrication of Polymeric Coatings. *Macromolecules* 2010;43:2413-2420.
21. Yuan W, Li CM. Exponentially growing layer-by-layer assembly to fabricate pH-responsive hierarchical nanoporous polymeric film and its superior controlled release performance. *Chem. Commun.* 2010;46:9161-9163.
22. Antipov AA, Sukhorukov GB, Donath E, Möhwald H. Sustained Release Properties of Polyelectrolyte Multilayer Capsules. *J. Phys. Chem. B* 2001;105:2281-2284.
23. Choi D, Hong J. Layer-by-layer assembly of multilayer films for controlled drug release. *ARCH PHARM RES.* 2014;37:79-87
24. Vergaro V, Scarlino F, Bellomo C, Rinaldi R, Vergara D, Maffia M, Baldassarre F, Giannelli G, Zhang X, Lvov YM, Leporatti S. Drug-loaded polyelectrolyte microcapsules for sustained targeting of cancer cells. *ADV DRUG DELIV REV.* 2011;63:847-864.

25. Volodkin D, Arntz Y, Schaaf P, Moehwald H, Voegel JC, Balla V. Composite multilayered biocompatible polyelectrolyte films with intact liposomes: stability and temperature triggered dye release. *Soft matter* 2007;4:122-130.
26. Matsuda M, Shiratori S, Correlation of Antithrombogenicity and Heat Treatment for Layer-by-Layer Self-Assembled Polyelectrolyte Films. *Langmuir* 2011;27:4271-4277.
27. Meng Sheng, Liu Zongjun, Shen Li. The effect of a layer-by-layer chitosan–heparin coating on the endothelialization and coagulation properties of a coronary stent system. *Biomaterials* 2009;30:2276-2283.
28. Shu Y, Ou G, Wang L, Zou J, Li Q. Surface Modification of Titanium with Heparin-Chitosan Multilayers via Layer-by-Layer Self-Assembly Technique. *Journal of Nanomaterials* 2011;423686.
29. Bulwan M, Zapotoczny S, Nowakowska M. Robust “one-component” chitosan-based ultrathin films fabricated using layer-by-layer technique. *Soft matter*, 2009;5:4726-4732.
30. Chen P, Lin AY, McKittrick J, Mayer MA. Structure and mechanical properties of crab exoskeletons. *Acta Biomater.* 2008;4:587-596.
31. Ifuku S, Nogi M, Abe K, Yoshioka M, Saimoto H, Yano H. Preparation of Chitin Nanofibers with a Uniform Width as r-Chitin from Crab Shells. *Biomacromolecules* 2009;10:1584-1588.
32. Serruys PW, van Hout B, Bonnier H, Legrand V, Garcia E, Macaya C, Sousa E, van der Giessen W, Colombo A, Seabra-Gomes R, Kiemeneij F, Ruygrok P, Ormiston J, Emanuelsson H, Fajadet J, Haude M, Klugmann S, Morel MA, Randomised. comparison of implantation of heparin-coated stents with balloon angioplasty in selected patients with coronary artery disease (Benestent II). *Lancet* 1998;352:673-81.
33. Serruys PW, Emanuelsson H, van der Giessen W, Lunn AC, Kiemeneij F, Macaya C, Rutsch W, Heyndrickx G, Suryapranata H, Legrand V, Goy JJ, Materne P, Bonnier H, Morice MC, Fajadet J, Belardi J, Colombo A, Garcia E, Ruygrok P, de Jaegere P, Morel MA. Heparin-coated Palmaz-Schatz stents in human coronary arteries. Early outcome of the Benestent-II Pilot Study. *Circulation* 1996;93:412-422.

34. Hårdhammar PA, van Beusekom HM, Emanuelsson HU, Hofma SH, Albertsson PA, Verdouw PD, Boersma E, Serruys PW, van der Giessen WJ. Reduction in thrombotic events with heparin-coated Palmaz-Schatz stents in normal porcine coronary arteries. *Circulation* 1996;93:423-430.
35. Shu Y, Yin P, Liang B, Wang S, Gao L, Wang H, Guo L. Layer by layer assembly of heparin/layered double hydroxide completely renewable ultrathin films with enhanced strength and blood compatibility. *Mater. Chem.* 2012;22:21667–21672.
36. Becker B, Cooper MA. A survey of the 2006–2009 quartz crystal microbalance biosensor literature. *J. Mol. Recognit.* 2011;24:754-787.
37. Cooper MA, Singleton VT. A survey of the 2001 to 2005 quartz crystal microbalance biosensor literature: applications of acoustic physics to the analysis of biomolecular interactions. *J. Mol. Recognit.* 2007;20:154-184.
38. Nair KG, Dufresne A. Crab Shell Chitin Whisker Reinforced Natural Rubber Nanocomposites. 1. Processing and Swelling Behavior. *Biomacromolecules* 2003;4:657-665.
39. Fan Y, Saito T, Isogai A. Individual chitin nano-whiskers prepared from partially deacetylated  $\alpha$ -chitin by fibril surface cationization. *Carbohydr. Polym.* 2010;79:1046–1051.
40. Kenji K, Gordon G. THE OSCILLATION FREQUENCY OF A QUARTZ RESONATOR IN CONTACT WITH A LIQUID. *ANALYT CHIM.* 1984;175:99-105.
41. Sauerbrey G, Verwendung von Schwingquarzen zur Waigung dünner Schichten und zur Mikrowaigung. *Z PHYS D.* 1959;155:206-222.
42. Findenig G, Kargl R, Stana-Kleinschek K, Ribitsch V. Interaction and Structure in Polyelectrolyte/Clay Multilayers: A QCM-D Study. *Langmuir* 2013;29:8544–8553.
43. Trojer MA, Li Y, Wallin M, Holmberg K, Nydén M. Charged microcapsules for controlled release of hydrophobic actives Part II: surface modification by LbL adsorption and lipid bilayer formation on properly anchored dispersant layers. *J Colloid Interface Sci.* 2013;409:8-17.

44. Fukada K, Taniguchi T, Shiratori S, Viscoelastic and durability analysis of nanostructured composite layers of polyelectrolyte and nanoparticles, RSC Adv., 2015, 5, 52837.

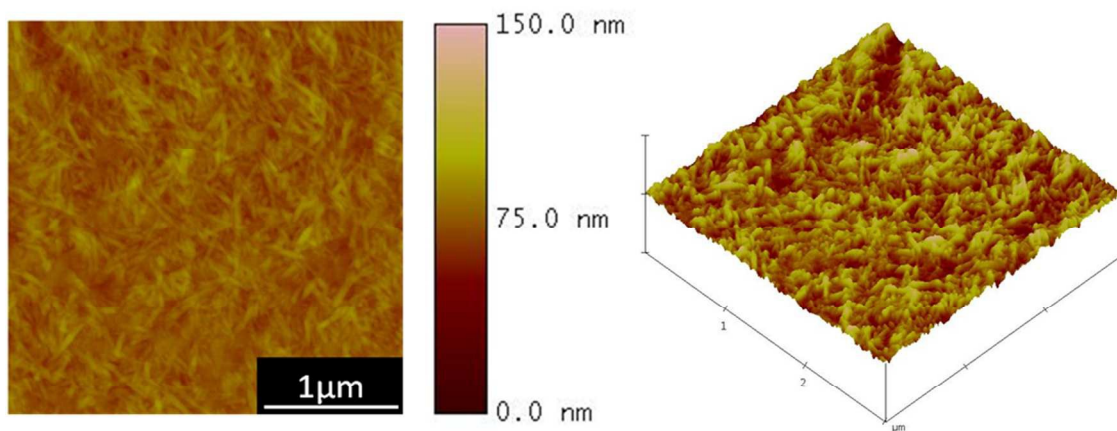


Fig.1 AFM image of the cast film of CHNFs

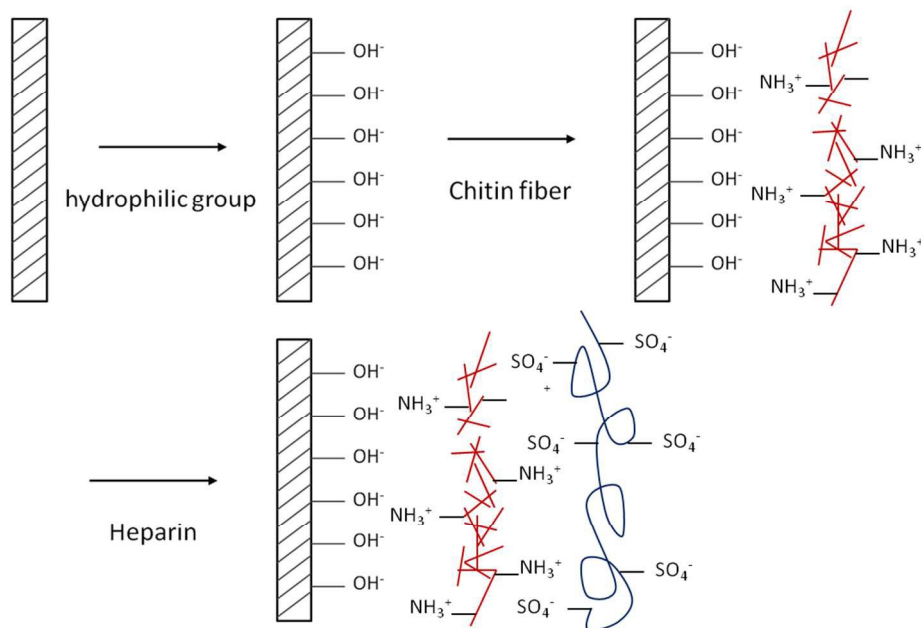


Fig.2 Schematic illustration of LbL self-assembly process with oppositely-charged CHNFs and HEP polyelectrolyte multilayers on a glass substrate

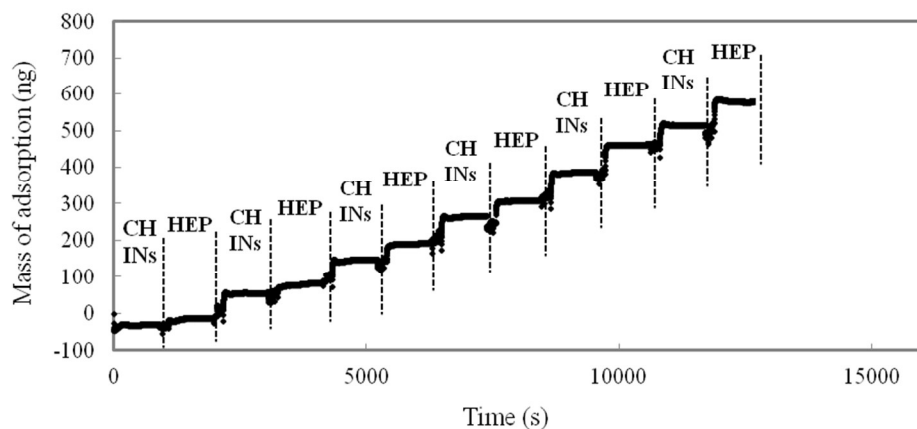


Fig.3 Mass of polyelectrolyte adsorption onto QCM substrate

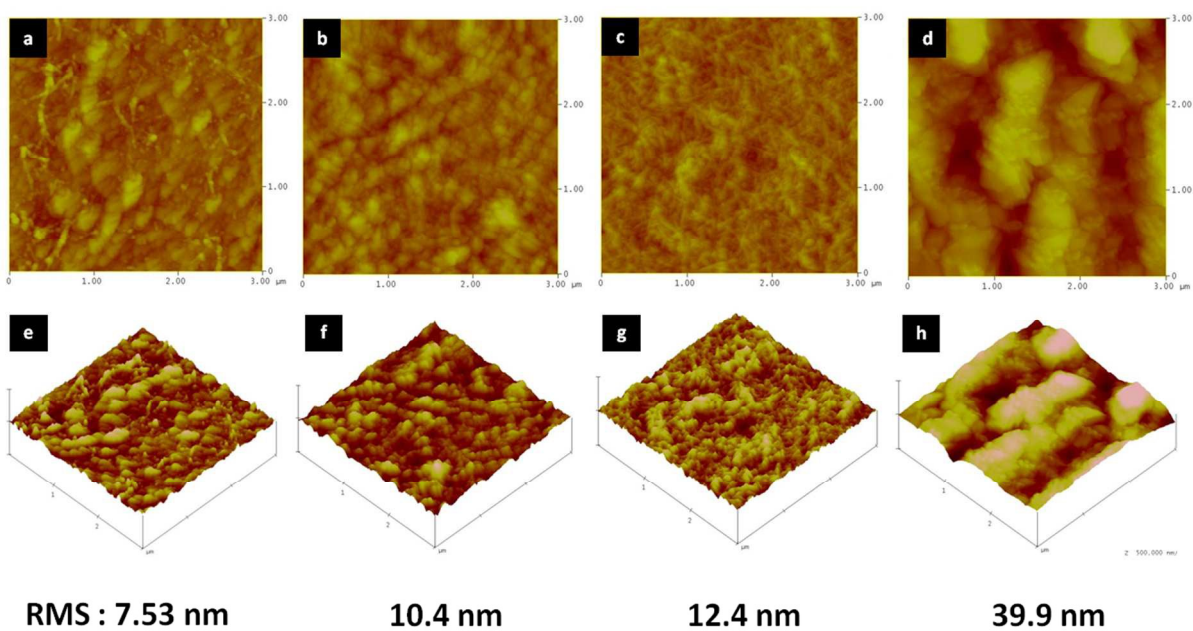


Fig.4 AFM images of (CHNFs / HEP) multilayers. (a) and (e): 10 bilayer, (b) and (f): 20 bilayer, (c) and (g): 30 bilayer, (d) and (h): 50 bilayer

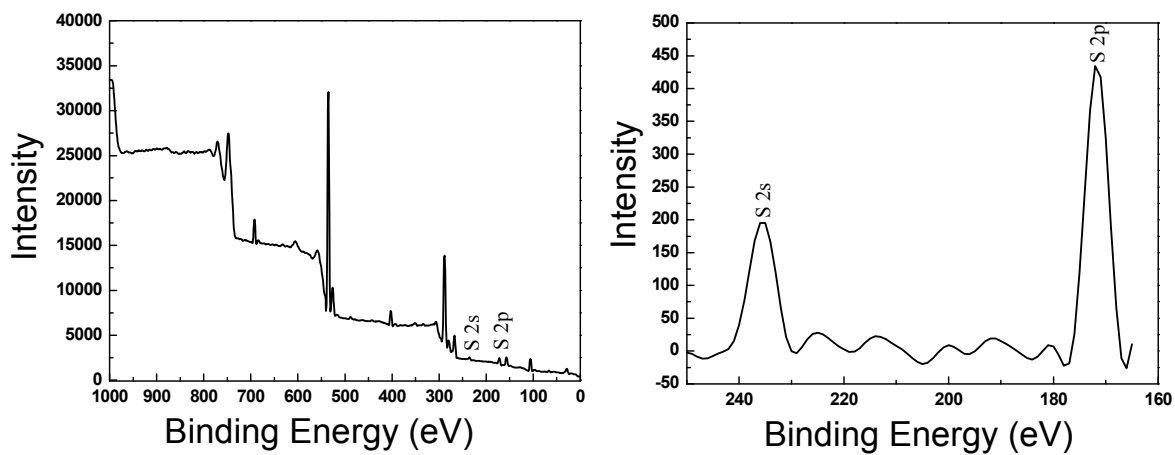


Fig.5 XPS spectra of (CHNFs / HEP)<sub>30</sub> multilayer film

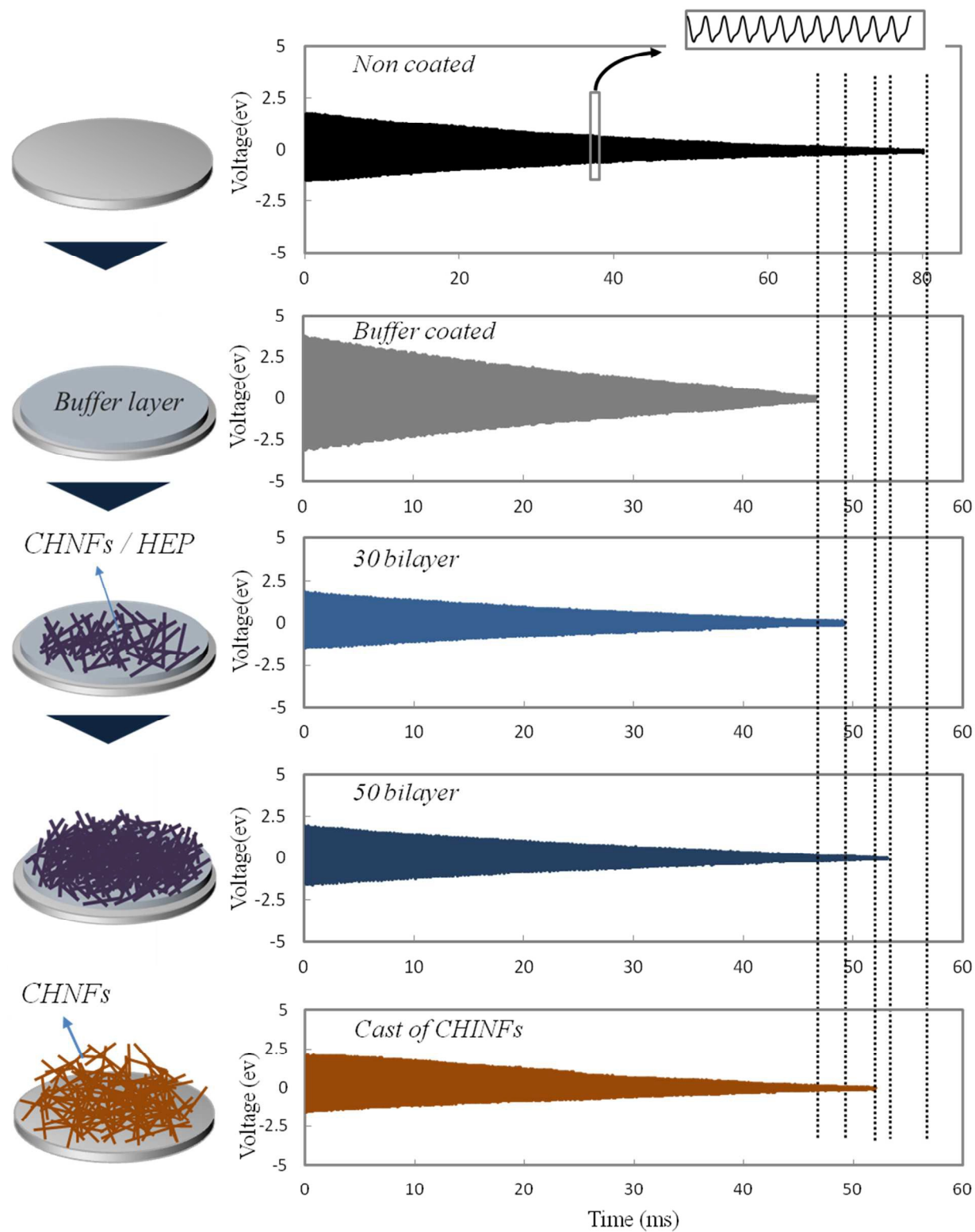
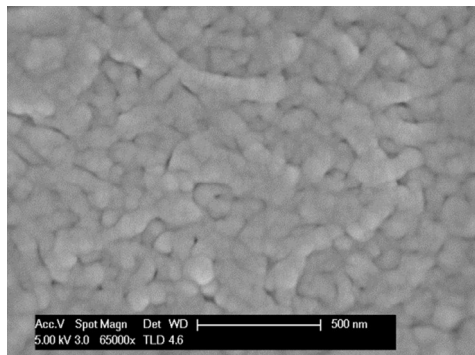
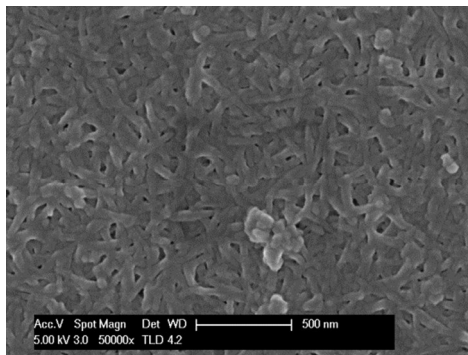


Fig.6 Damping waves of oscillating circuit for QCM substrates

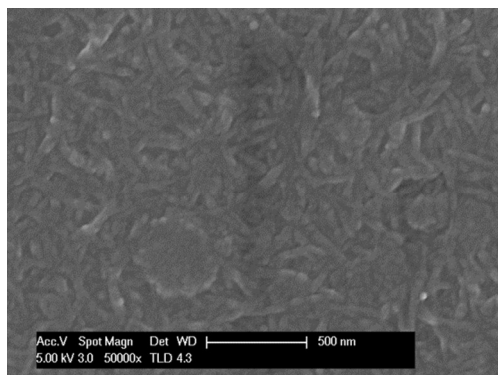
(a)



(b)



(c)



(d)

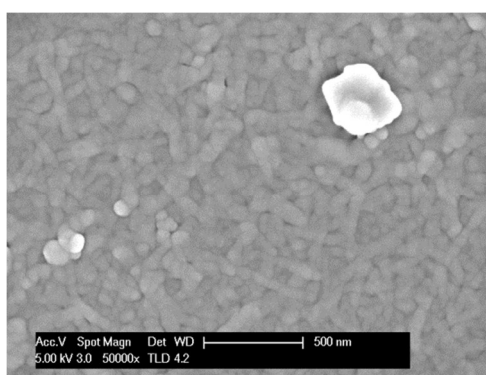


Fig.7 SEM images of the (CHNFs/HEP)<sub>30</sub> multilayer film after immersion in PBS for: (a) 0 h, (b) 3 h, (c) 6 h, and (d) 48 h

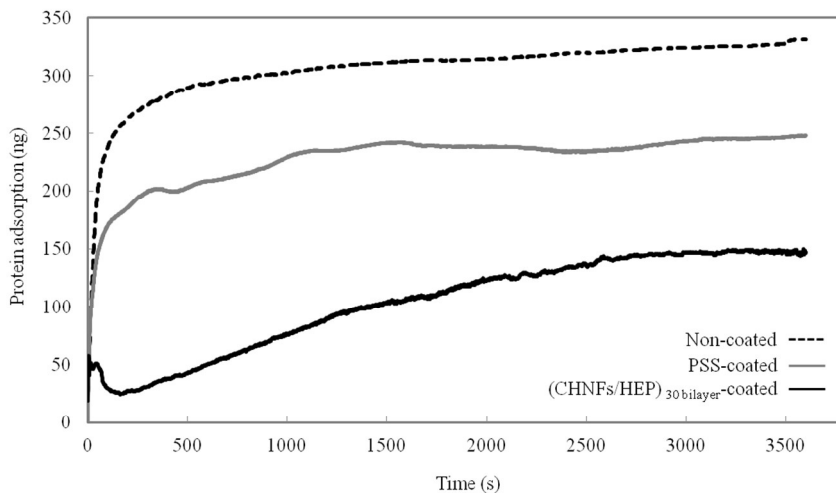


Fig.8 Mass of fibrinogens adsorbed onto the QCM substrates

The black solid line is for the (CHNFs/HEP)<sub>30</sub>-coated QCM substrate. The dashed line and gray solid line are non-coated and buffer-only-coated (top layer is PSS layer) QCM substrates, respectively.

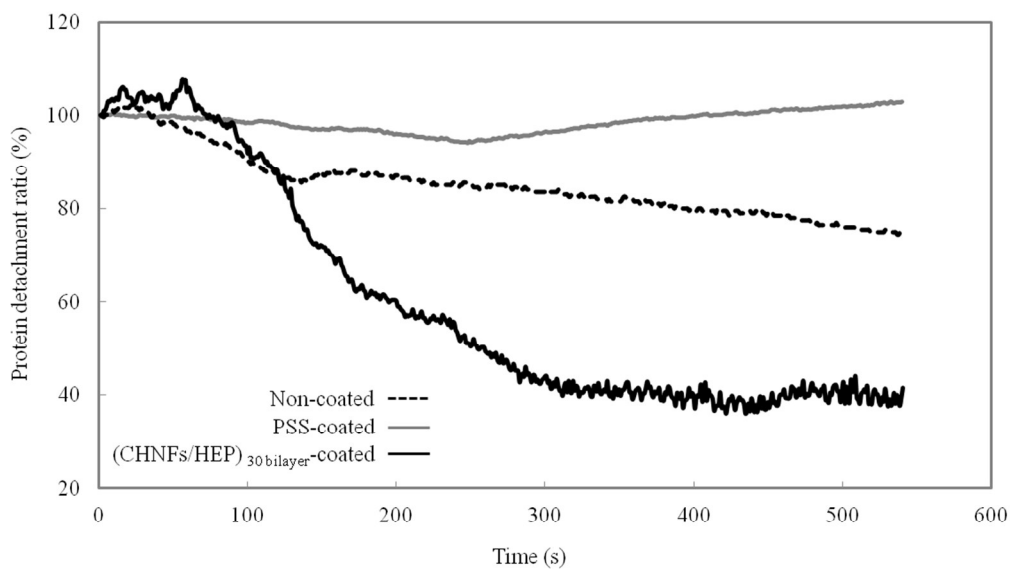


Fig.9 Detachment ratio of absorbed fibrinogens from QCM s upon rinsing with ultra-pure water

The black solid line is for the (CHNFs/HEP)<sub>30</sub>-coated QCM substrate; the dashed line and gray solid line are for the non-coated and buffer-only-coated (the top layer is PSS layer) QCM substrates, respectively.

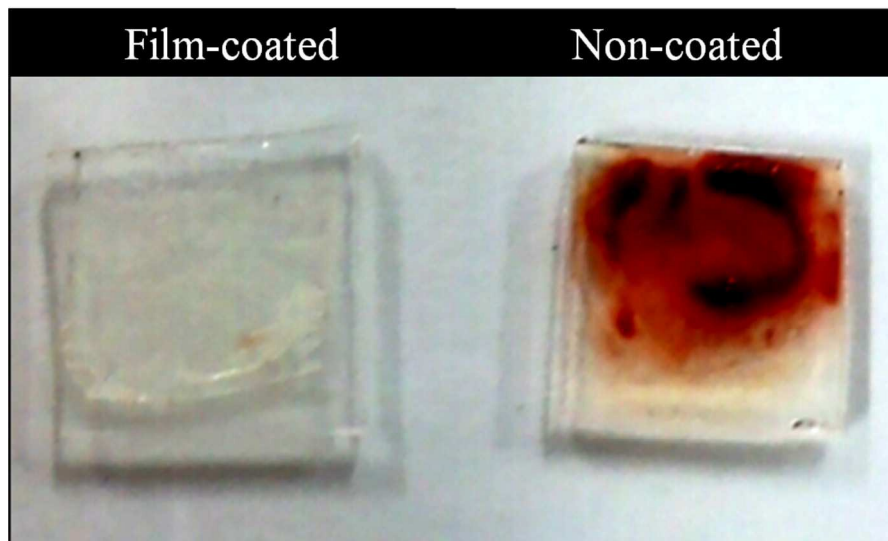


Fig.10 Adhesion of blood to coated and uncoated 1×1cm glass substrates

#### Table of Contents

Layer-by-layer assembled film of chitin nanofibers and heparin with anti-thrombus characteristics

